Supporting information

Role of Double Interfaces in Inspiring Energy Storage Devices in CC@Ni(OH)Cl@NiO Flexible Electrodes

Sixian Fu,[a] Liping Li,[a] Lingshen Meng,[a] Mengyue Gao,[a] Shuaikai Xu,[b] Xiyang Wang,[a] Yuelan Zhang[a] and Guangshe Li[a]*

[a] State Key Laboratory of Inorganic Synthesis and Preparative Chemistry, College of Chemistry, Jilin University, Changchun 130012, P.R. China

[b] Key Laboratory of Physics and Technology for Advanced Batteries, Ministry of Education, Jilin University, Changchun 130012, P.R. China

*E-mail: guangshe@jlu.edu.cn.

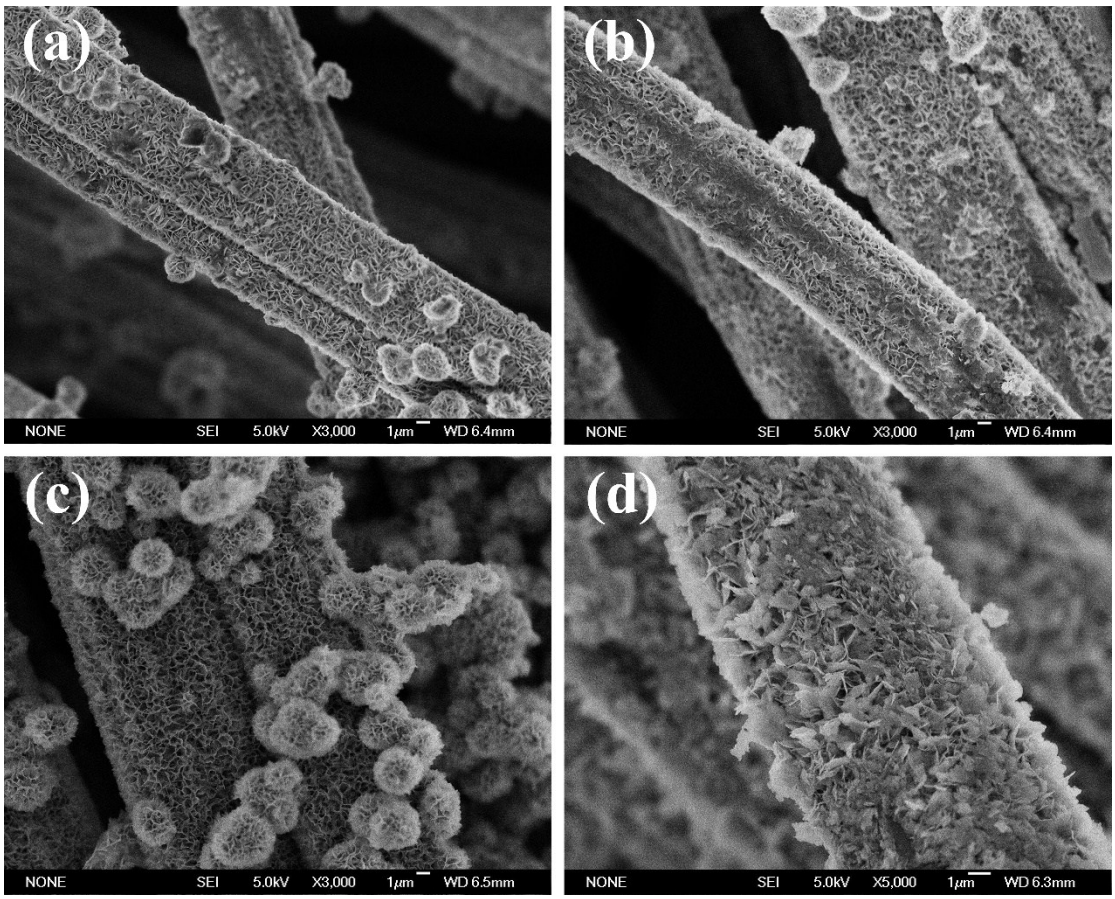

Fig. S1 SEM images of CC@Ni(OH)Cl synthesized by different solvothermal conditions: (a) 10 mmol $NiCl_2 \cdot 6H_2O$ precursor reacted at 140 °C for 12 h; (b) 10 mmol $NiCl_2 \cdot 6H_2O$ precursor reacted at 160 °C for 12 h; (c) 6 mmol $NiCl_2 \cdot 6H_2O$ precursor reacted at 180 °C for 12 h; (d) 10 mmol $NiCl_2 \cdot 6H_2O$ precursor reacted at 200 °C for 12 h.

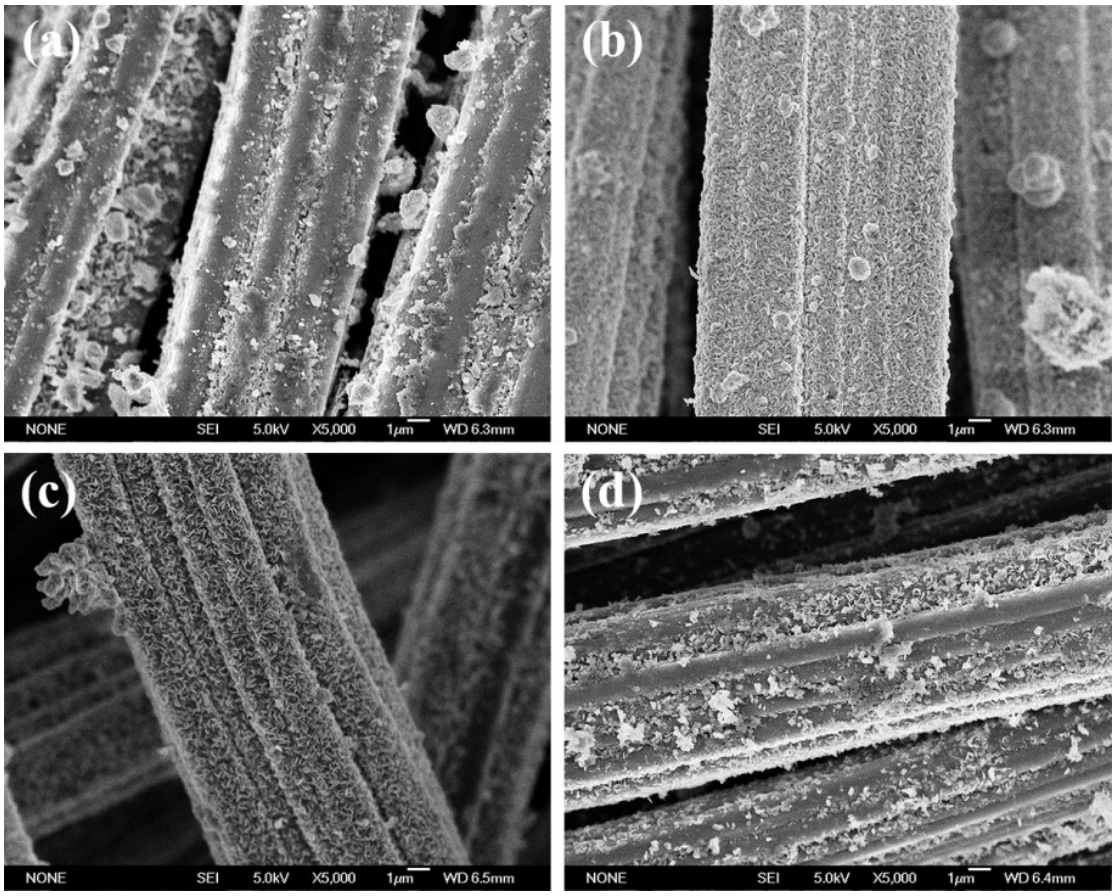

Fig. S2 SEM images of CC@Ni(OH)NO_3 synthesized by different solvothermal conditions: (a) 12 mmol $Ni(NO_3)_2 \cdot 6H_2O$ precursor reacted at 180 ^oC for 12 h; (b) 14 mmol $Ni(NO_3)_2 \cdot 6H_2O$ precursor reacted at 180 ^oC for 12 h; (c) 10 mmol $Ni(NO_3)_2 \cdot 6H_2O$ precursor reacted at 200 ^oC for 12 h; (d) 10 mmol $Ni(NO_3)_2 \cdot 6H_2O$ precursor reacted at 160 ^oC for 12 h.

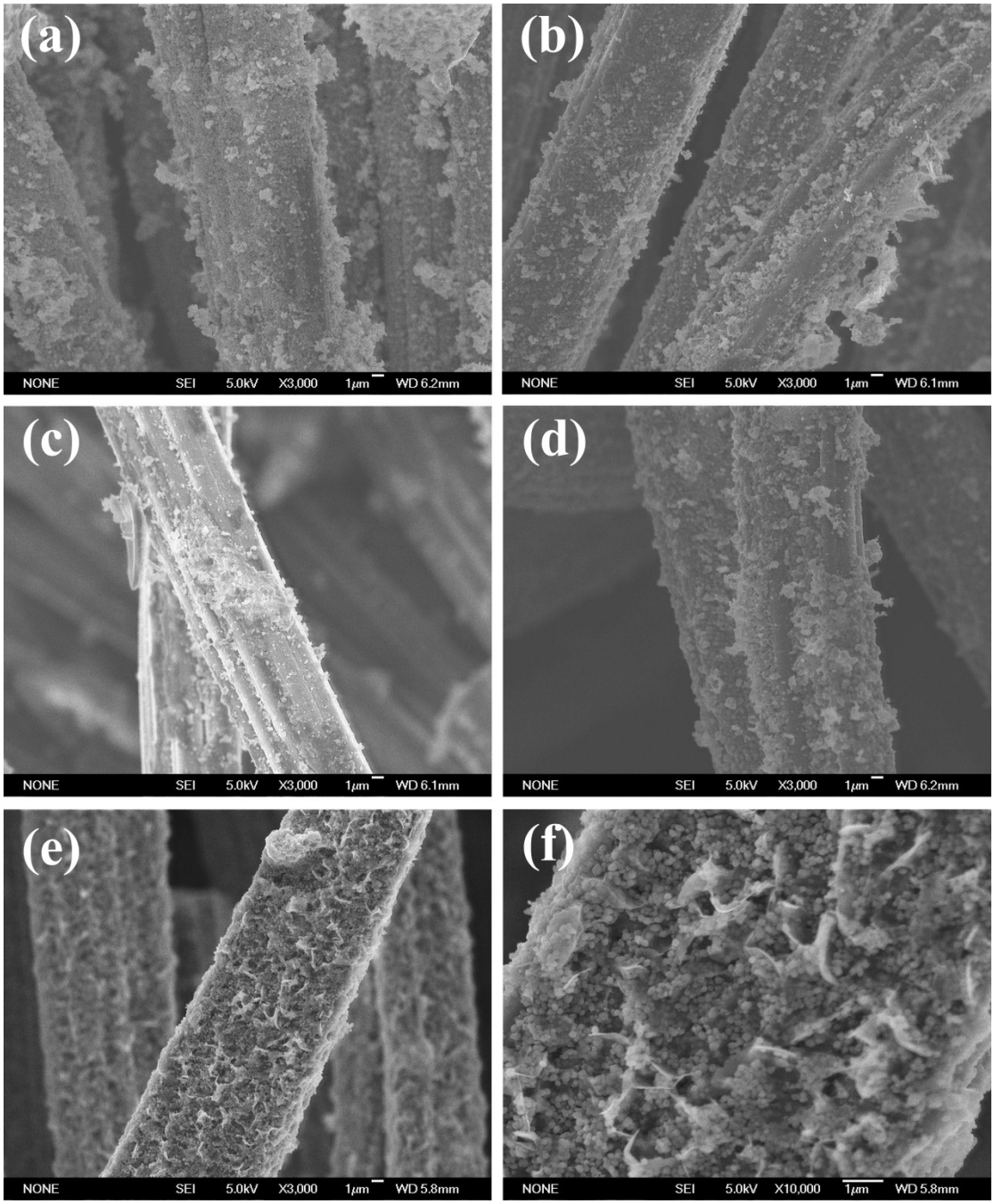

Fig. S3 SEM images of CC@Ni(OH)CH_3COO synthesized by different solvothermal conditions: (a) 10 mmol $Ni(CH_3COO)_2 \cdot 4H_2O$ precursor reacted at 140 ^oC for 12 h; (b) 10 mmol $Ni(CH_3COO)_2 \cdot 4H_2O$ precursor reacted at 160 ^oC for 12 h; (c) 10 mmol $Ni(CH_3COO)_2 \cdot 4H_2O$ precursor reacted at 200 ^oC for 12 h; (d) 10 mmol $Ni(CH_3COO)_2 \cdot 4H_2O$ precursor reacted at 180 ^oC for 24 h; (e-f) 10 mmol $Ni(CH_3COO)_2 \cdot 4H_2O$ precursor reacted at 180 ^oC for 12 h.

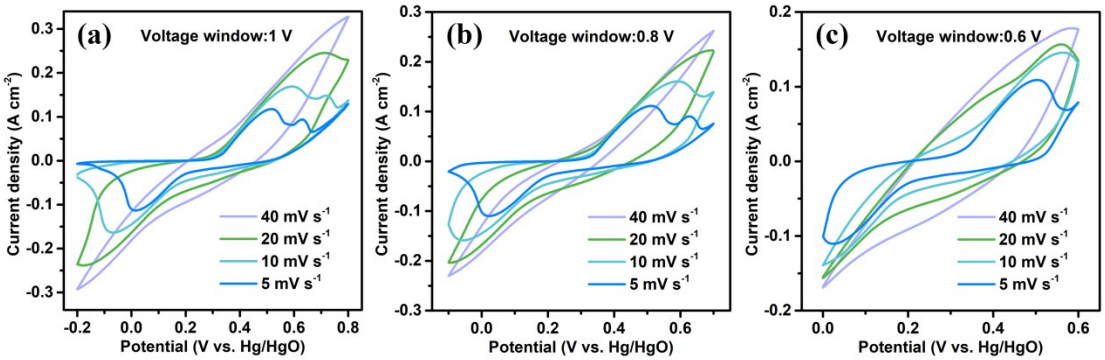

Fig. S4 CV curves of CC@Ni(OH)Cl@NiO electrode with scan rates from 5 to 40 mV s^{-1} in various voltage windows: (a) 1 V, (b) 0.8 V, and (c) 0.6 V.

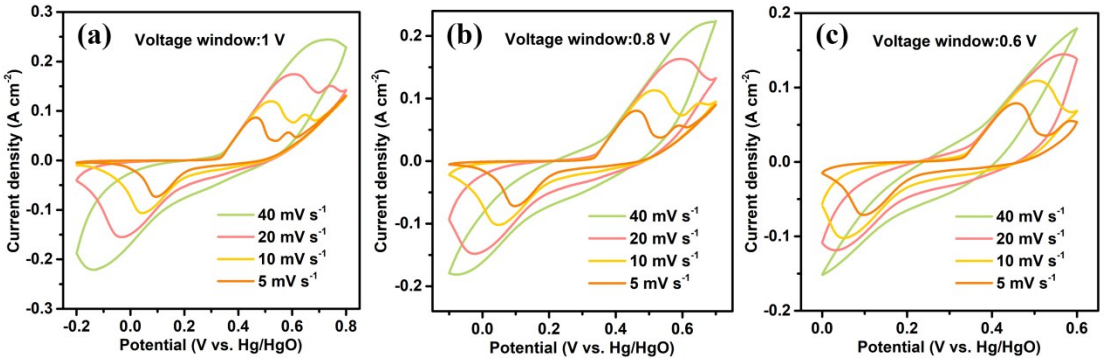

Fig. S5 CV curves of CC@Ni(OH)Cl electrode with scan rates from 5 to 40 mV s^{-1} in various voltage windows: (a) 1 V, (b) 0.8 V, and (c) 0.6 V.

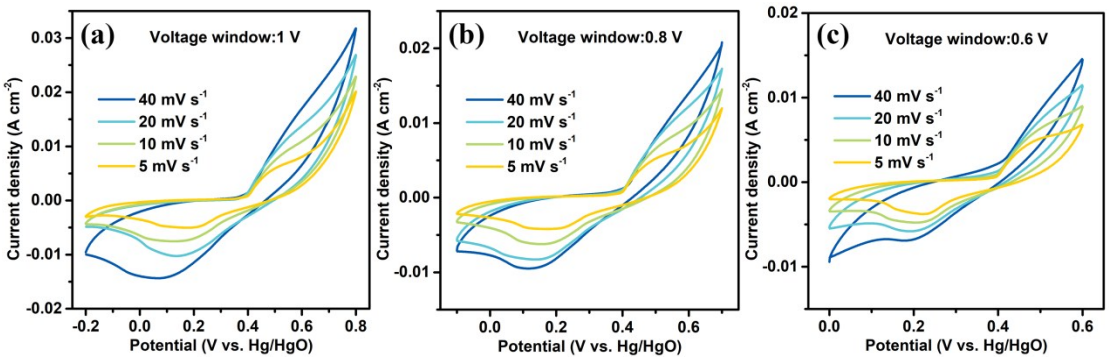

Fig. S6 CV curves of Ni(OH)Cl pasted on CC electrode with scan rates from 5 to 40 mV s^{-1} in various voltage windows: (a) 1 V, (b) 0.8 V, and (c) 0.6 V.

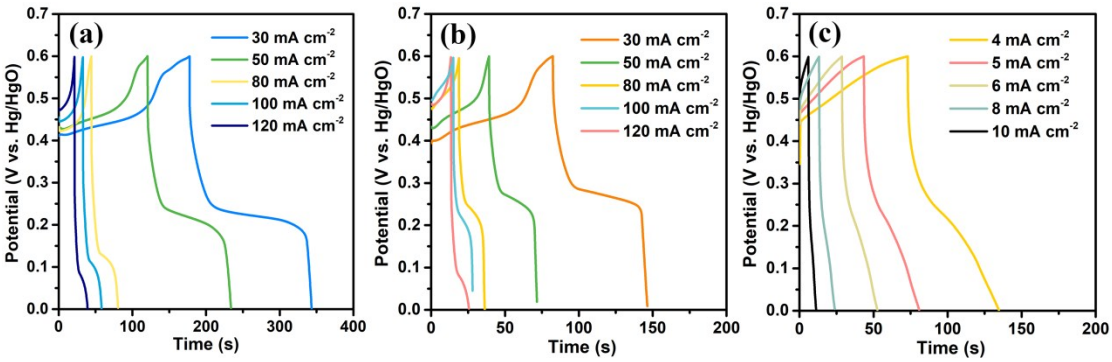

Fig. S7 GCD curves under various current densities: (a) CC@Ni(OH)Cl@NiO, (b) CC@Ni(OH)Cl, and (c) Ni(OH)Cl pasted on CC.

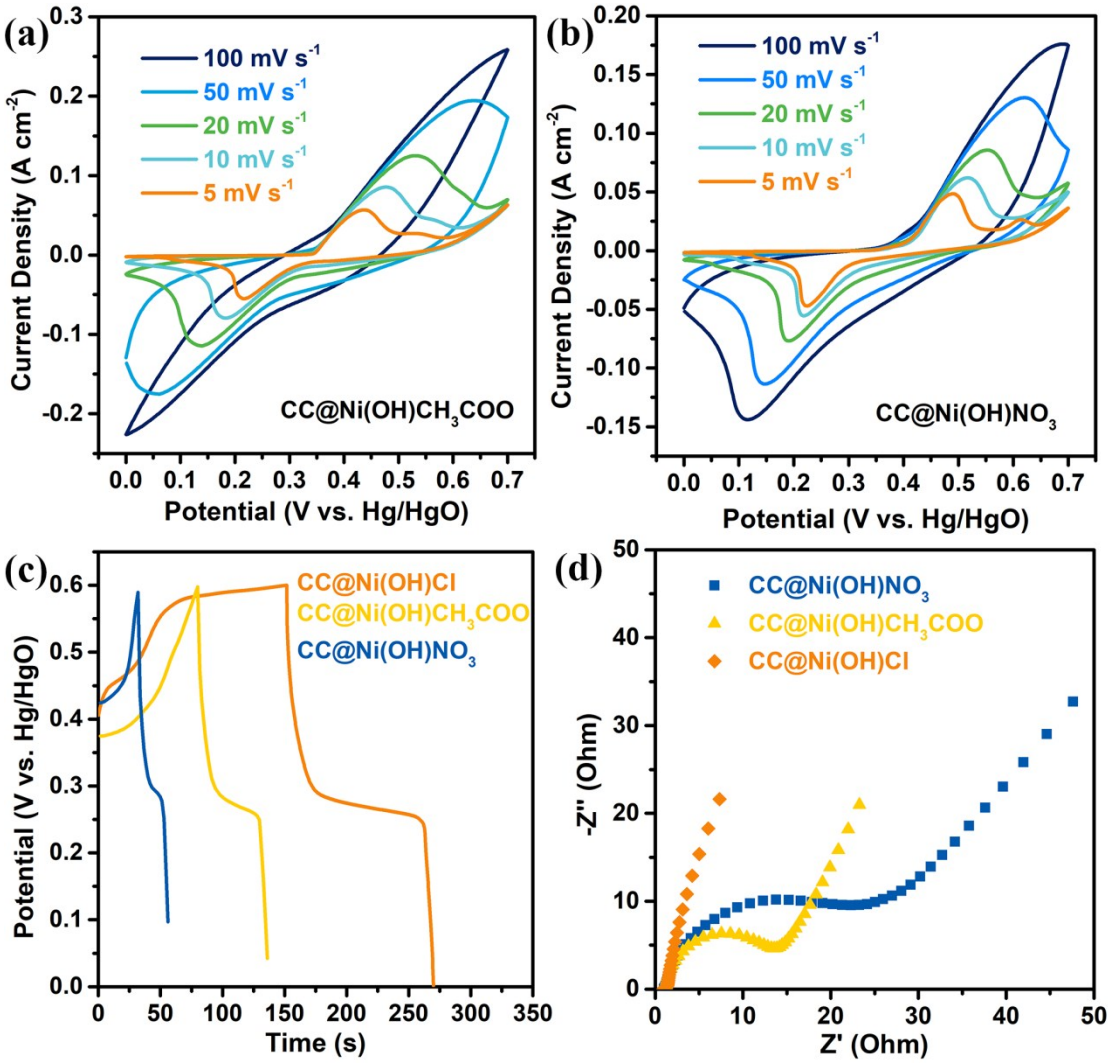

Fig. S8 (a) CV curves of CC@Ni(OH)CH_3COO electrode at various scan rates; (b) CV curves of CC@Ni(OH)NO_3 electrode at various scan rates; (c) Comparative GCD curves of CC@Ni(OH)Cl, CC@Ni(OH)CH_3COO, and CC@Ni(OH)NO_3 electrodes at 20 mA cm^{-2}; (d) Nyquist plots of CC@Ni(OH)Cl, CC@Ni(OH)CH_3COO, and CC@Ni(OH)Cl@NiO electrodes.

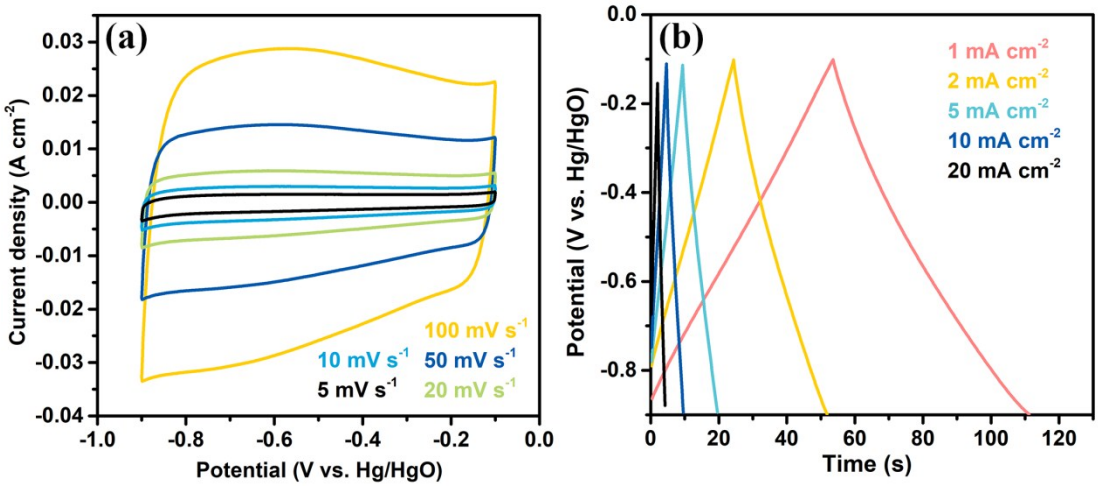

Fig. S9 (a) CV curves of graphene on CC electrode at various scan rates; (b) GCD curves of graphene on CC electrode under different current densities.

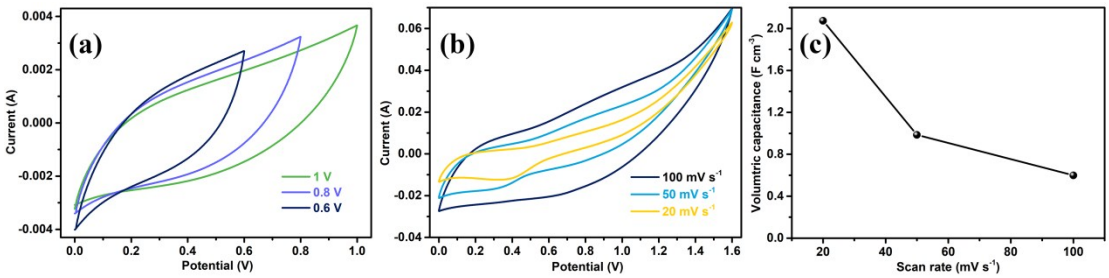

Fig. S10 (a) CV curves of CC@Ni(OH)Cl@NiO//graphene device at potential window from 0.6 V to 1 V; (b) CV curves of CC@Ni(OH)Cl@NiO//graphene device at various scan rates; (c) Volumetric capacitance of CC@Ni(OH)Cl@NiO//graphene device under various scan rates.

Table S1 Comparison of capacitive performance for double-interface CC@Ni(OH)Cl@NiO with recently reported Ni-based flexible electrodes.

Material	**Electrolyte (KOH concentration)**	**Reference**	**Current density (mA cm^{-2})**	**Areal capacitance (F cm^{-2})**	**Current density (A g^{-1})**	**Specific capacitance (F g^{-1})**
CC@Ni(OH)Cl@NiO	6 M	This work	30 120	8.29 3.58	8 32	2241 968
Ni-Co@Ni-Co LDH NTAs/CFC	1 M	1	4.6	2.0	5	2200
Co-Ni LDH/PWC	6 M	2	-	1.076	5	1592.76
NiMoO4@Ni-Co-S	2 M	3	5	2.27	-	1892
Ni-decorated Co_9S_8	6 M	4	1	5.64	-	-
Ni-Co-S/ACC	6 M	5	-	-	1	2392
$Ni(OH)_2$–MnO_2/C composite	6 M	6	- -	- -	2 40	862 574

References

1 Y. Liu, N. Fu, G. Zhang, M. Xu, W. Lu, L. Zhou and H. Huang, *Adv. Funct. Mater.*, 2017, **27**, 1605307.

2 X. Liang, G. Long, C. Fu, M. Pang, Y. Xi, J. Li, W. Han, G. Wei and Y. Ji, *Chem. Eng. J.*, 2018, **345**, 186-195.

3 C. Chen, D. Yan, X. Luo, W. Gao, G. Huang, Z. Han, Y. Zeng and Z. Zhu, *ACS Appl. Mater. Interfaces*, 2018, **10**, 4662-4671.

4 Y. Wen, Y. Liu, S. Dang, S. Tian, H. Li, Z. Wang, D. He, Z.-S. Wu, G. Cao and S. Peng, *J. Power Sources*, 2019, **423**, 106-114.

5 W. Zhao, Y. Zheng, L. Cui, D. Jia, D. Wei, R. Zheng, C. Barrow, W. Yang and J. Liu, *Chem. Eng. J.*, 2019, **371**, 461-469.

6 X. Xu, W. Shi, W. Liu, S. Ye, R. Yin, L. Zhang, L. Xu, M. Chen, M. Zhong and X. Cao, *J. Mater. Chem. A*, 2018, **6**, 24086-24091.